Extracting Macroscopic Data from Microscopic Images -

grain boundaries and macroscopic deformations from images on atomic scale

Martin Rumpf, Bonn University

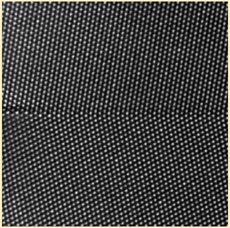

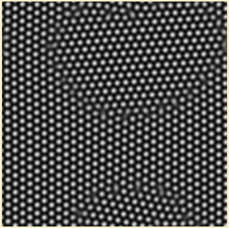

Image Analysis Challenges in Molecular Microscopy, January 28 - February 1, 2008

joint work with:

B. Berkels, O. Nemitz (Bonn),
A. Rätz, A. Voigt (Dresden)

macroscopic parameters from microscopic observations

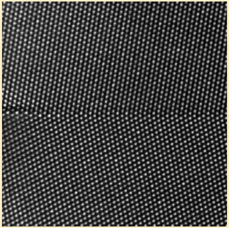

transmission electron microscopy (courtesy G.H. Campell, Lawrence Livermore Nat. Lab.)

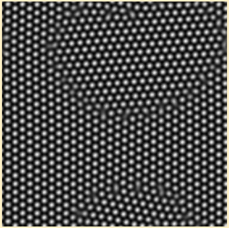

phase field cristal simulation [Rätz, Voigt '06]

macroscopic parameters from microscopic observations

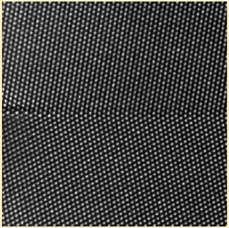

transmission electron microscopy
(courtesy G.H. Campell,
Lawrence Livermore Nat. Lab.)

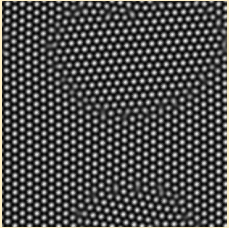

phase field cristal simulation
[Rätz, Voigt '06]

aim: identification of grain boundary contours, orientations, and macroscopic deformation fields

macroscopic parameters from microscopic observations

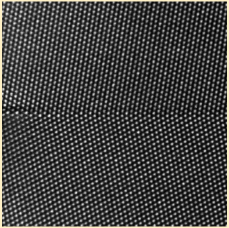

transmission electron microscopy (courtesy G.H. Campell, Lawrence Livermore Nat. Lab.)

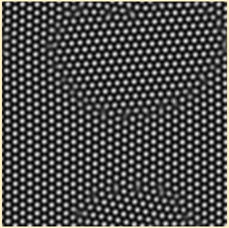

phase field cristal simulation [Rätz, Voigt '06]

aim: identification of grain boundary contours, orientations, and macroscopic deformation fields
$\longrightarrow$ a generalized Mumford Shah approach

Recall: Mumford Shah free discontinuity problem

Given $g : \Omega \to \mathbb{R}$ find an set $S \subset \Omega$ and a piecewise smooth $u : \Omega \setminus S \to \mathbb{R}$ such that

$$E[u, S] = \int_\Omega (u - g)^2 \,\mathrm{d}x + \mu \int_{\Omega \setminus S} |\nabla u|^2 \,\mathrm{d}x + \nu \mathcal{H}^{d-1}(S)$$

is minimized.

[Mumford, Shah '86]

Recall: Mumford Shah free discontinuity problem

universitätbonn

Given $g : \Omega \to \mathbb{R}$ find an set $S \subset \Omega$ and a piecewise smooth $u : \Omega \setminus S \to \mathbb{R}$ such that

$$E[u, S] = \int_\Omega (u - g)^2 \, \mathrm{d}x + \mu \int_{\Omega \setminus S} |\nabla u|^2 \, \mathrm{d}x + \nu \mathcal{H}^{d-1}(S)$$

is minimized.

[Mumford, Shah '86]

Shape optimization perspective

Suppose Ω is partitioned into domains $\mathcal{O}_i$ $(i = 1, \ldots, m)$ with $\Omega = \bigcup_{i=1}^m \mathcal{O}_i \, , \quad \mathcal{O}_i \cap \mathcal{O}_j = \emptyset$ and consider

Recall: Mumford Shah free discontinuity problem

universitätbonn

Given $g : \Omega \to \mathbb{R}$ find an set $S \subset \Omega$ and a piecewise smooth $u : \Omega \setminus S \to \mathbb{R}$ such that

$$E[u, S] = \int_\Omega (u - g)^2 \, \mathrm{d}x + \mu \int_{\Omega \setminus S} |\nabla u|^2 \, \mathrm{d}x + \nu \mathcal{H}^{d-1}(S)$$

is minimized.

[Mumford, Shah '86]

Shape optimization perspective

Suppose Ω is partitioned into domains $\mathcal{O}_i$ $(i = 1, \dots, m)$ with $\Omega = \bigcup_{i=1}^m \mathcal{O}_i$, $\quad \mathcal{O}_i \cap \mathcal{O}_j = \emptyset$ and consider

$$S = \bigcup_{i=1}^m \partial \mathcal{O}_i$$

Recall: Mumford Shah free discontinuity problem

Given $g : \Omega \to \mathbb{R}$ find an set $S \subset \Omega$ and a piecewise smooth $u : \Omega \setminus S \to \mathbb{R}$ such that

$$E[u, S] = \int_\Omega (u - g)^2 \, \mathrm{d}x + \mu \int_{\Omega \setminus S} |\nabla u|^2 \, \mathrm{d}x + \nu \mathcal{H}^{d-1}(S)$$

is minimized.

[Mumford, Shah '86]

Shape optimization perspective

Suppose Ω is partitioned into domains $\mathcal{O}_i$ $(i = 1, \ldots, m)$ with $\Omega = \bigcup_{i=1}^m \mathcal{O}_i$, $\quad \mathcal{O}_i \cap \mathcal{O}_j = \emptyset$ and consider

$$S = \bigcup_{i=1}^m \partial \mathcal{O}_i \, , \quad u_i = u[\mathcal{O}_i] = u\big|_{\mathcal{O}_i} \, .$$

Recall: Mumford Shah free discontinuity problem

Given $g : \Omega \to \mathbb{R}$ find an set $S \subset \Omega$ and a piecewise smooth $u : \Omega \setminus S \to \mathbb{R}$ such that

$$E[u, S] = \int_\Omega (u-g)^2 \,\mathrm{d}x + \mu \int_{\Omega\setminus S} |\nabla u|^2 \,\mathrm{d}x + \nu \mathcal{H}^{d-1}(S)$$

is minimized.

[Mumford, Shah '86]

Shape optimization perspective

Suppose Ω is partitioned into domains $\mathcal{O}_i$ $(i = 1, \ldots, m)$ with $\Omega = \bigcup_{i=1}^m \mathcal{O}_i$, $\quad \mathcal{O}_i \cap \mathcal{O}_j = \emptyset$ and consider

$$S = \bigcup_{i=1}^m \partial\mathcal{O}_i \,, \quad u_i = u[\mathcal{O}_i] = u\big|_{\mathcal{O}_i} \,.$$

Then we ask for a minimizing partition $(\mathcal{O}_i)_{i=1,\ldots,m}$ of

$$E[(\mathcal{O}_i)_{i=1,\ldots,m}] = E[(u[\mathcal{O}_i], \mathcal{O}_i)_{i=1,\ldots,m}]$$

General structure of the Mumford Shah functional

$$E[(u_i,\mathcal{O}_i)_i] = \sum_i \left(E_{\text{fid}}[u_i,\mathcal{O}_i] + E_{\text{prior},u}[u_i,\mathcal{O}_i] + E_{\text{prior},\mathcal{O}}[\mathcal{O}_i]\right)$$

where	$(\mathcal{O}_i)_i$	is a domain partition
	u_i	a parameter (function) on $\mathcal{O}_i$

General structure of the Mumford Shah functional

$$E[(u_i,\mathcal{O}_i)_i] = \sum_i \left(E_{\text{fid}}[u_i,\mathcal{O}_i] + E_{\text{prior},u}[u_i,\mathcal{O}_i] + E_{\text{prior},\mathcal{O}}[\mathcal{O}_i]\right)$$

where $(\mathcal{O}_i)_i$ is a domain partition
u_i a parameter (function) on $\mathcal{O}_i$

"region competition": different local descriptors u_i compete for terrain [Zhu, Yuille '96]

General structure of the Mumford Shah functional

$$E[(u_i, \mathcal{O}_i)_i] = \sum_i \left(E_{\text{fid}}[u_i, \mathcal{O}_i] + E_{\text{prior},u}[u_i, \mathcal{O}_i] + E_{\text{prior},\mathcal{O}}[\mathcal{O}_i]\right)$$

where $(\mathcal{O}_i)_i$ is a domain partition
u_i a parameter (function) on $\mathcal{O}_i$

"region competition": different local descriptors u_i compete for terrain [Zhu, Yuille '96]

in our generalized Mumford Shah approach:

General structure of the Mumford Shah functional

$$E[(u_i,\mathcal{O}_i)_i] = \sum_i \left(E_{\text{fid}}[u_i,\mathcal{O}_i] + E_{\text{prior},u}[u_i,\mathcal{O}_i] + E_{\text{prior},\mathcal{O}}[\mathcal{O}_i]\right)$$

where $(\mathcal{O}_i)_i$ is a domain partition
u_i a parameter (function) on $\mathcal{O}_i$

"region competition": different local descriptors u_i compete for terrain [Zhu, Yuille '96]

in our generalized Mumford Shah approach:

- a macroscopic orientation parameter describes the microscopic lattice anisotropy

General structure of the Mumford Shah functional

$$E[(u_i, \mathcal{O}_i)_i] = \sum_i \left(E_{\text{fid}}[u_i, \mathcal{O}_i] + E_{\text{prior},u}[u_i, \mathcal{O}_i] + E_{\text{prior},\mathcal{O}}[\mathcal{O}_i]\right)$$

where $(\mathcal{O}_i)_i$ is a domain partition
u_i a parameter (function) on $\mathcal{O}_i$

"region competition": different local descriptors u_i compete for terrain [Zhu, Yuille '96]

in our generalized Mumford Shah approach:

- a macroscopic orientation parameter describes the microscopic lattice anisotropy
- a macroscopic deformation influences the lattice pattern

Some related work on pattern analysis

- unsupervised texture segmentation using markov random fields [Manjunath, Chellappa '91]

Some related work on pattern analysis

- unsupervised texture segmentation using markov random fields [Manjunath, Chellappa '91]
- texture classification using Wavelets [Unser '95]

Some related work on pattern analysis

- unsupervised texture segmentation using markov random fields [Manjunath, Chellappa '91]
- texture classification using Wavelets [Unser '95]
- BV^*, BV decomposition [Meyer '01]

Some related work on pattern analysis

- unsupervised texture segmentation using markov random fields [Manjunath, Chellappa '91]
- texture classification using Wavelets [Unser '95]
- BV^*, BV decomposition [Meyer '01]
- combining level sets and Gabor filter for texture analysis [Chan, Vese, Osher '02]

Some related work on pattern analysis

- unsupervised texture segmentation using markov random fields [Manjunath, Chellappa '91]
- texture classification using Wavelets [Unser '95]
- BV^*, BV decomposition [Meyer '01]
- combining level sets and Gabor filter for texture analysis [Chan, Vese, Osher '02]
- Numerical approx. of BV^*, BV decomposition [Vese, Osher '03]

Some related work on pattern analysis

- unsupervised texture segmentation using markov random fields [Manjunath, Chellappa '91]
- texture classification using Wavelets [Unser '95]
- BV^*, BV decomposition [Meyer '01]
- combining level sets and Gabor filter for texture analysis [Chan, Vese, Osher '02]
- Numerical approx. of BV^*, BV decomposition [Vese, Osher '03]
- dynamic texture segmention [Doretto, Cremers, Favaro, Soatto '03]

Some related work on pattern analysis

- unsupervised texture segmentation using markov random fields [Manjunath, Chellappa '91]
- texture classification using Wavelets [Unser '95]
- BV^*, BV decomposition [Meyer '01]
- combining level sets and Gabor filter for texture analysis [Chan, Vese, Osher '02]
- Numerical approx. of BV^*, BV decomposition [Vese, Osher '03]
- dynamic texture segmention [Doretto, Cremers, Favaro, Soatto '03]
- wavelet texture analysis [Aujol et al. '06]

Some related work on pattern analysis

- unsupervised texture segmentation using markov random fields [Manjunath, Chellappa '91]
- texture classification using Wavelets [Unser '95]
- BV^*, BV decomposition [Meyer '01]
- combining level sets and Gabor filter for texture analysis [Chan, Vese, Osher '02]
- Numerical approx. of BV^*, BV decomposition [Vese, Osher '03]
- dynamic texture segmention [Doretto, Cremers, Favaro, Soatto '03]
- wavelet texture analysis [Aujol et al. '06]
- combining geometric and texture information [Aujol, Chan '06]

Some related work on pattern analysis

- unsupervised texture segmentation using markov random fields [Manjunath, Chellappa '91]
- texture classification using Wavelets [Unser '95]
- BV^*, BV decomposition [Meyer '01]
- combining level sets and Gabor filter for texture analysis [Chan, Vese, Osher '02]
- Numerical approx. of BV^*, BV decomposition [Vese, Osher '03]
- dynamic texture segmention [Doretto, Cremers, Favaro, Soatto '03]
- wavelet texture analysis [Aujol et al. '06]
- combining geometric and texture information [Aujol, Chan '06]
- ...

An energy based on local pattern classification

description of the lattice:

An energy based on local pattern classification

description of the lattice:

x	atom position
$x + M(\alpha) q_i$	neighbour locations $(i = 1, \cdots, m)$

$$M(\alpha) := \begin{pmatrix} \cos\alpha & -\sin\alpha \\ \sin\alpha & \cos\alpha \end{pmatrix}$$

$\left[\text{e.g. } q_i := d\left(\cos\left(i\frac{\pi}{3}\right), \sin\left(i\frac{\pi}{3}\right)\right)\right]$

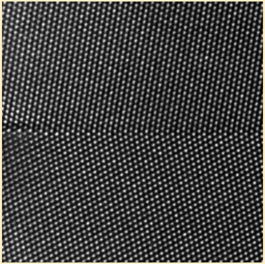

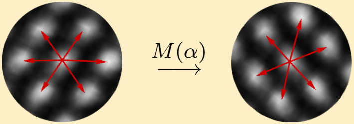

An energy based on local pattern classification

description of the lattice:

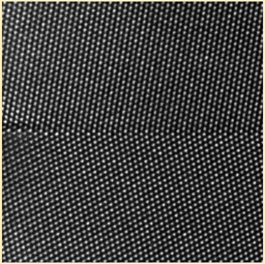

x	atom position
$x + M(\alpha) q_i$	neighbour locations $(i = 1, \cdots, m)$

$$M(\alpha) := \begin{pmatrix} \cos\alpha & -\sin\alpha \\ \sin\alpha & \cos\alpha \end{pmatrix}$$

$$\left[\text{e.g. } q_i := d\left(\cos\left(i\tfrac{\pi}{3}\right), \sin\left(i\tfrac{\pi}{3}\right)\right)\right]$$

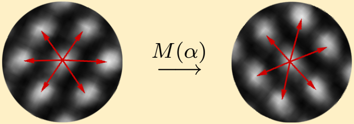

indicator function for atomic dots:

$$\chi_{[u>\theta]}(x) := \begin{cases} 1; & u(x) > \theta \\ 0; & \text{else} \end{cases}$$

An energy based on local pattern classification (cont.)

description of the lattice:

x atom position

$x + M(\alpha)q_i$ neighbour locations $(i = 1, \cdots, m)$

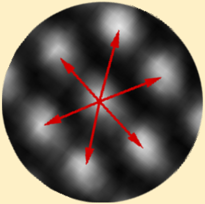

local lattice classification function:

An energy based on local pattern classification (cont.)

description of the lattice:

x	atom position
$x + M(\alpha)q_i$	neighbour locations $(i = 1, \cdots, m)$

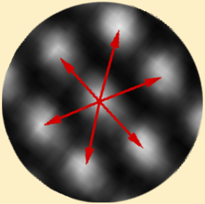

local lattice classification function:

$$f[\alpha](x) = \frac{d^2}{m\,r^2} \chi_{[u>\theta]}(x) \sum_{i=1}^{m} (1 - \chi_{[u>\theta]}(x + M(\alpha)q_i)) \,,$$

where	d	distance between atom dots,
	m	number of neighbouring dots,
	r	dot radius.

An energy based on local pattern classification (cont.)

macroscopic lattice orientation function:

$$\alpha = \sum_{j=1,\cdots,n} \alpha_j \chi_{\mathcal{O}_j}$$

An energy based on local pattern classification (cont.)

macroscopic lattice orientation function:

$$\alpha = \sum_{j=1,\cdots,n} \alpha_j \chi_{\mathcal{O}_j}$$

Mumford Shah type functional E_{grain} acting on lattice orientations α_j and grain domains $\mathcal{O}_j$:

$$E_{\mathsf{grain}}[(\alpha_j, \mathcal{O}_j)_{j=1,\cdots,n}] = \sum_{j=1,\cdots,n} \left(\int_{\mathcal{O}_j} f[\alpha_j](x)\,\mathrm{d}x + \frac{\nu}{2}\mathcal{H}^1(\partial\mathcal{O}_j) \right),$$

An energy based on local pattern classification (cont.)

macroscopic lattice orientation function:

$$\alpha = \sum_{j=1,\cdots,n} \alpha_j \chi_{\mathcal{O}_j}$$

Mumford Shah type functional E_{grain} acting on lattice orientations α_j and grain domains $\mathcal{O}_j$:

$$E_{\text{grain}}[(\alpha_j, \mathcal{O}_j)_{j=1,\cdots,n}] = \sum_{j=1,\cdots,n} \left(\int_{\mathcal{O}_j} f[\alpha_j](x)\, \mathrm{d}x + \frac{\nu}{2} \mathcal{H}^1(\partial \mathcal{O}_j) \right),$$

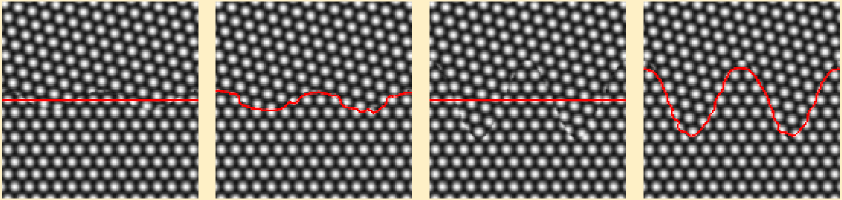

An energy based on local pattern classification (cont.)

direct consequences of the variational approach:

- relation between interface curvature on $\mathcal{O}_j \cap \mathcal{O}_k$ and fidelity term:

  $\nu\kappa = -(f[\alpha_j] - f[\alpha_k])$

  $0 \leq f[\alpha] \leq \frac{d^2}{r^2} \Rightarrow |\kappa| \leq \frac{d^2}{\nu r^2}$

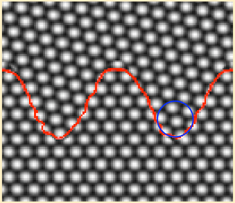

An energy based on local pattern classification (cont.)

direct consequences of the variational approach:

- relation between interface curvature on $\mathcal{O}_j \cap \mathcal{O}_k$ and fidelity term:

  $\nu\kappa = -(f[\alpha_j] - f[\alpha_k])$

  $0 \leq f[\alpha] \leq \frac{d^2}{r^2} \Rightarrow |\kappa| \leq \frac{d^2}{\nu r^2}$

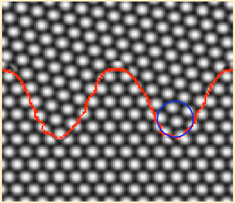

- Young's law at triple points, i.e. three grains always meet at equal angles of $\frac{2}{3}\pi$.

Recall: Chan-Vese approximation

Recall: Chan-Vese approximation

for the original Mumford Shah functional

$$E[u,S] = \int_\Omega (u-g)^2 \,\mathrm{d}x + \mu \int_{\Omega\setminus S} |\nabla u|^2 \,\mathrm{d}x + \nu \mathcal{H}^{d-1}(S)$$

in the piecewise constant case with $S = \partial\mathcal{O}_1 \cup \partial\mathcal{O}_2$, $u|_{\mathcal{O}_i} \equiv$ const

Recall: Chan-Vese approximation

for the original Mumford Shah functional

$$E[u,S] = \int_\Omega (u-g)^2 \,\mathrm{d}x + \mu \int_{\Omega\setminus S} |\nabla u|^2 \,\mathrm{d}x + \nu \mathcal{H}^{d-1}(S)$$

in the piecewise constant case with $S = \partial\mathcal{O}_1 \cup \partial\mathcal{O}_2$, $u|_{\mathcal{O}_i} \equiv$ const
we consider $\mathcal{O}_1 = [\phi < 0] = [H(\phi) = 0]\,,\ \overline{\mathcal{O}_2} = [H(\phi) = 1]$
(H heavyside fct.)

Recall: Chan-Vese approximation

for the original Mumford Shah functional

$$E[u,S] = \int_\Omega (u-g)^2 \,\mathrm{d}x + \mu \int_{\Omega\setminus S} |\nabla u|^2 \,\mathrm{d}x + \nu \mathcal{H}^{d-1}(S)$$

in the piecewise constant case with $S = \partial\mathcal{O}_1 \cup \partial\mathcal{O}_2$, $u|_{\mathcal{O}_i} \equiv$ const
we consider $\mathcal{O}_1 = [\phi < 0] = [H(\phi) = 0]$, $\overline{\mathcal{O}_2} = [H(\phi) = 1]$
(H heavyside fct.) and reformulate

$$E[u_1,u_2,\phi] = \int_\Omega H(\phi)((u_2-g)^2 + \mu|\nabla u_2|^2) + (1-H(\phi))((u_1-g)^2 + \mu|\nabla u_1|^2)\,\mathrm{d}x + \nu|D\,H(\phi)|(\Omega)$$

cf. [Vese, Chan '99]

Recall: Chan-Vese approximation

universitätbonn

for the original Mumford Shah functional

$$E[u,S] = \int_\Omega (u-g)^2 \,\mathrm{d}x + \mu \int_{\Omega\setminus S} |\nabla u|^2 \,\mathrm{d}x + \nu \mathcal{H}^{d-1}(S)$$

in the piecewise constant case with $S = \partial\mathcal{O}_1 \cup \partial\mathcal{O}_2$, $u|_{\mathcal{O}_i} \equiv$ const
we consider $\mathcal{O}_1 = [\phi < 0] = [H(\phi) = 0]\,,\ \overline{\mathcal{O}_2} = [H(\phi) = 1]$
(H heavyside fct.) and approximate

$$E_\delta[u_1,u_2,\phi] = \int_\Omega H_\delta(\phi)(u_2-g)^2 + \mu|\nabla u_2|^2 + (1-H_\delta(\phi))(u_1-g)^2 + \mu|\nabla u_1|^2 + \nu|\nabla H_\delta(\phi)|\,\mathrm{d}x$$

where $H_\delta(s) = \frac{1}{2} + \frac{1}{\pi}\arctan(\frac{x}{\delta})$.

cf. [Vese, Chan '99]

Grain boundary extraction by a Chan-Vese approach

regularized lattice classification function:

$$f_\epsilon[\alpha](X) = \frac{d^2}{m\, r^2} H_\epsilon(u(x) - \theta) \sum_{i=1,\cdots,m} (1 - (H_\epsilon(u(x + M(\alpha)q_i) - \theta)))$$

$\longrightarrow$ to be motivated later

Grain boundary extraction by a Chan-Vese approach

regularized lattice classification function:

$$f_\epsilon[\alpha](X) = \frac{d^2}{m\,r^2} H_\epsilon(u(x)-\theta) \sum_{i=1,\cdots,m} (1-(H_\epsilon(u(x+M(\alpha)q_i)-\theta)))$$

$\longrightarrow$ to be motivated later

in the two grain case we obtain the approximate functional:

$$E_{\delta,\epsilon}[\alpha_1,\alpha_2,\phi] \quad = \quad \int_\Omega H_\delta(\phi) f_\epsilon[\alpha_2] + (1-H_\delta(\phi)) f_\epsilon[\alpha_1]$$

$$+\nu|\nabla H_\delta(\phi)|\,\mathrm{d}x$$

Grain boundary extraction by a Chan-Vese approach

universitätbonn

regularized lattice classification function:

$$f_\epsilon[\alpha](X) = \frac{d^2}{m\, r^2} H_\epsilon(u(x) - \theta) \sum_{i=1,\cdots,m} (1 - (H_\epsilon(u(x + M(\alpha)q_i) - \theta)))$$

$\longrightarrow$ to be motivated later

in the two grain case we obtain the approximate functional:

$$\begin{aligned} E_{\delta,\epsilon}[\alpha_1, \alpha_2, \phi] \; &= \; \int_\Omega H_\delta(\phi) f_\epsilon[\alpha_2] + (1 - H_\delta(\phi)) f_\epsilon[\alpha_1] \\ &\qquad + \nu |\nabla H_\delta(\phi)| \, \mathrm{d}x \end{aligned}$$

where two types of regularization are involved:

- regularization parameter δ for the macroscopic interfaces

Grain boundary extraction by a Chan-Vese approach

regularized lattice classification function:

$$f_\epsilon[\alpha](X) = \frac{d^2}{m\,r^2} H_\epsilon(u(x)-\theta) \sum_{i=1,\cdots,m} (1 - (H_\epsilon(u(x+M(\alpha)q_i) - \theta)))$$

$\longrightarrow$ to be motivated later

in the two grain case we obtain the approximate functional:

$$E_{\delta,\epsilon}[\alpha_1,\alpha_2,\phi] = \int_\Omega H_\delta(\phi) f_\epsilon[\alpha_2] + (1 - H_\delta(\phi)) f_\epsilon[\alpha_1] + \nu |\nabla H_\delta(\phi)| \,\mathrm{d}x$$

where two types of regularization are involved:

- regularization parameter δ for the macroscopic interfaces
- regularization parameter ϵ for the microscopic interfaces ($\epsilon \leq \delta$)

Numerical relaxation with regularized gradient descent

the functional to be minimized:

$$E_{\delta,\epsilon}[\alpha_1,\alpha_2,\phi] = \int_\Omega H_\delta(\phi) f_\epsilon[\alpha_2] + (1 - H_\delta(\phi)) f_\epsilon[\alpha_1] + \nu |\nabla H_\delta(\phi)| \,\mathrm{d}x$$

Numerical relaxation with regularized gradient descent

the functional to be minimized:

$$E_{\delta,\epsilon}[\alpha_1,\alpha_2,\phi] = \int_\Omega H_\delta(\phi) f_\epsilon[\alpha_2] + (1 - H_\delta(\phi)) f_\epsilon[\alpha_1] + \nu |\nabla H_\delta(\phi)| \,\mathrm{d}x$$

Algorithm (in the two grain case):

Numerical relaxation with regularized gradient descent

the functional to be minimized:

$$E_{\delta,\epsilon}[\alpha_1, \alpha_2, \phi] = \int_\Omega H_\delta(\phi) f_\epsilon[\alpha_2] + (1 - H_\delta(\phi)) f_\epsilon[\alpha_1] + \nu |\nabla H_\delta(\phi)| \,\mathrm{d}x$$

Algorithm (in the two grain case):

- for fixed $\Phi^k \in \mathcal{V}_h$ update α_1^k, α_2^k via a discrete version of

$$\alpha_1^{k+1} = \alpha_1^k - \tau \int_\Omega H_\delta(\phi) \partial_{\alpha_1} f_\epsilon[\alpha_1^k]$$

Numerical relaxation with regularized gradient descent

the functional to be minimized:

$$E_{\delta,\epsilon}[\alpha_1,\alpha_2,\phi] = \int_\Omega H_\delta(\phi) f_\epsilon[\alpha_2] + (1-H_\delta(\phi)) f_\epsilon[\alpha_1] + \nu |\nabla H_\delta(\phi)| \,\mathrm{d}x$$

Algorithm (in the two grain case):

- for fixed $\Phi^k \in \mathcal{V}_h$ update α_1^k, α_2^k via a discrete version of

$$\begin{aligned} \alpha_1^{k+1} &= \alpha_1^k - \tau \int_\Omega H_\delta(\phi) \partial_{\alpha_1} f_\epsilon[\alpha_1^k] \\ \alpha_2^{k+1} &= \alpha_2^k - \tau \int_\Omega (1 - H_\delta(\phi)) \partial_{\alpha_2} f_\epsilon[\alpha^k] \end{aligned}$$

Numerical relaxation with regularized gradient descent

the functional to be minimized:

$$E_{\delta,\epsilon}[\alpha_1,\alpha_2,\phi] = \int_\Omega H_\delta(\phi) f_\epsilon[\alpha_2] + (1 - H_\delta(\phi)) f_\epsilon[\alpha_1] + \nu |\nabla H_\delta(\phi)| \,\mathrm{d}x$$

Algorithm (in the two grain case):

- for fixed $\Phi^k \in \mathcal{V}_h$ update α_1^k, α_2^k via a discrete version of

$$\begin{aligned} \alpha_1^{k+1} &= \alpha_1^k - \tau \int_\Omega H_\delta(\phi) \partial_{\alpha_1} f_\epsilon[\alpha_1^k] \\ \alpha_2^{k+1} &= \alpha_2^k - \tau \int_\Omega (1 - H_\delta(\phi)) \partial_{\alpha_2} f_\epsilon[\alpha^k] \end{aligned}$$

- for given $\alpha_{1,2}^k$ compute $\Phi^k \in \mathcal{V}_h$ via a discrete time step of:

$$g\left(H_\delta'(\phi)^{-1} \partial_t \phi, \theta \right) = \int_\Omega \nu \frac{\nabla \phi}{|\nabla \phi|} \nabla \theta + (f_\epsilon[\alpha_1^k] - f_\epsilon[\alpha_2^k]) \theta \,\mathrm{d}x \,,$$

Numerical relaxation with regularized gradient descent

the functional to be minimized:

$$E_{\delta,\epsilon}[\alpha_1,\alpha_2,\phi] = \int_\Omega H_\delta(\phi) f_\epsilon[\alpha_2] + (1 - H_\delta(\phi)) f_\epsilon[\alpha_1] + \nu |\nabla H_\delta(\phi)| \,\mathrm{d}x$$

Algorithm (in the two grain case):

- for fixed $\Phi^k \in \mathcal{V}_h$ update α_1^k, α_2^k via a discrete version of

$$\begin{aligned} \alpha_1^{k+1} &= \alpha_1^k - \tau \int_\Omega H_\delta(\phi) \partial_{\alpha_1} f_\epsilon[\alpha_1^k] \\ \alpha_2^{k+1} &= \alpha_2^k - \tau \int_\Omega (1 - H_\delta(\phi)) \partial_{\alpha_2} f_\epsilon[\alpha^k] \end{aligned}$$

- for given $\alpha_{1,2}^k$ compute $\Phi^k \in \mathcal{V}_h$ via a discrete time step of:

$$g\left(H'_\delta(\phi)^{-1} \partial_t \phi, \theta\right) = \int_\Omega \nu \frac{\nabla \phi}{|\nabla \phi|} \nabla \theta + (f_\epsilon[\alpha_1^k] - f_\epsilon[\alpha_2^k]) \theta \,\mathrm{d}x \,,$$

where $g(\xi_1,\xi_2) = \int_\Omega \xi_1(x)\xi_2(x) + \frac{\sigma^2}{2} \nabla \xi_1(x) \cdot \nabla \xi_2(x) \,\mathrm{d}x$

Grain boundary extraction on TEM images

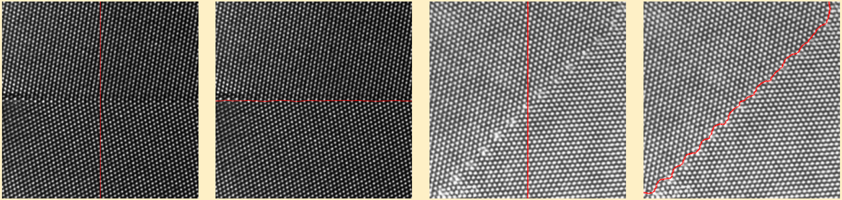

[Berkels, Rätz, R., Voigt '06]

Grain boundary extraction on TEM images (cont.)

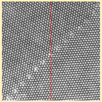

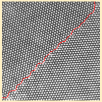

energy decay plot:

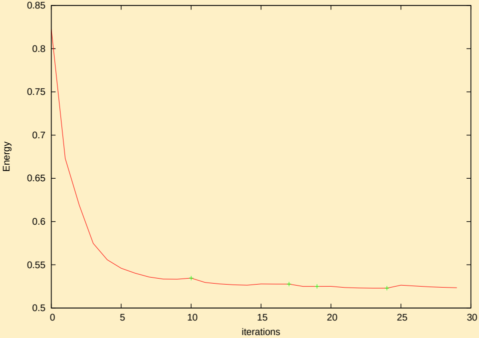

The crosses mark refinements of the scale parameter σ.

Multi–phase grain boundary extraction

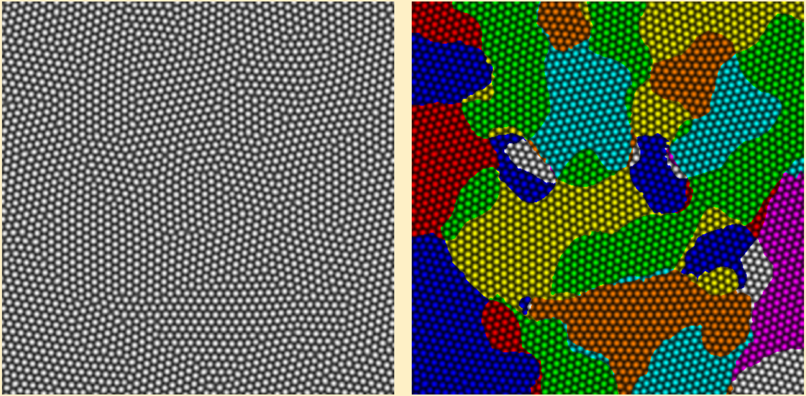

Segmentation with multiple grains using three level set functions

[Vese, Chan '02]

An additional liquid–solid interface

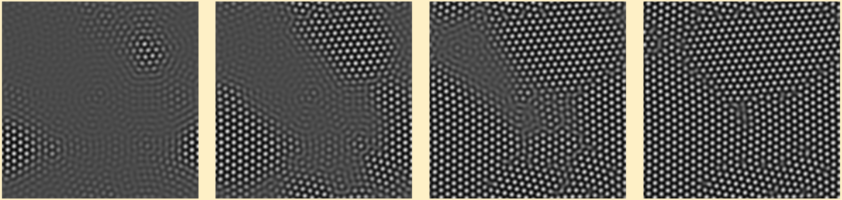

liquid / crystal and grain interface evolution [Rätz, Voigt '06]

An additional liquid–solid interface

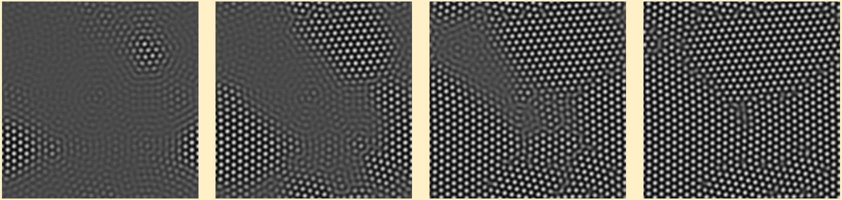

liquid / crystal and grain interface evolution [Rätz, Voigt '06]

local classification based on the image:

description of the liquid phase: $u(x) \in [\theta_1, \theta_2]$ and $|\nabla u(x)| < \gamma$

An additional liquid–solid interface

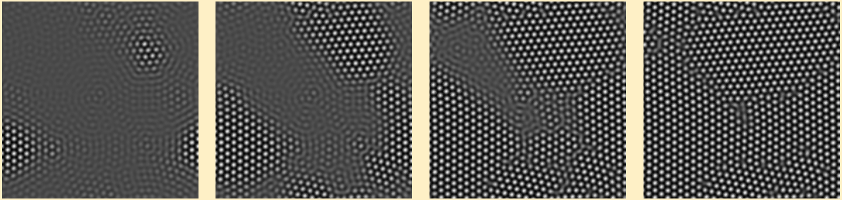

liquid / crystal and grain interface evolution [Rätz, Voigt '06]

local classification based on the image:

description of the liquid phase: $u(x) \in [\theta_1, \theta_2]$ and $|\nabla u(x)| < \gamma$

Incorporating a liquid–solid interface (cont)

local liquid classification function:

$$g(x) = 1 - \chi_{[u>\theta_1]}(x)\chi_{[u<\theta_2]}(x)\chi_{[|\nabla u|<\gamma]}(x)$$

Incorporating a liquid–solid interface (cont)

local liquid classification function:

$$g(x) = 1 - \chi_{[u>\theta_1]}(x)\chi_{[u<\theta_2]}(x)\chi_{[|\nabla u|<\gamma]}(x)$$

Mumford Shah type functional E_{phase} acting on liquid domain $\mathcal{O}_L$:

$$E_{\text{phase}}[\mathcal{O}_L] = \int\limits_{\mathcal{O}_L} 1 - g(x)\,\mathrm{d}x + \int\limits_{\Omega\setminus\mathcal{O}_L} g(x)\,\mathrm{d}x + \nu\mathcal{H}^1(\mathcal{O}_L)$$

Incorporating a liquid–solid interface (cont)

local liquid classification function:

$$g(x) = 1 - \chi_{[u>\theta_1]}(x)\chi_{[u<\theta_2]}(x)\chi_{[|\nabla u|<\gamma]}(x)$$

Mumford Shah type functional E_{phase} acting on liquid domain $\mathcal{O}_L$:

$$E_{\text{phase}}[\mathcal{O}_L] = \int_{\mathcal{O}_L} 1 - g(x)\,\mathrm{d}x + \int_{\Omega\setminus\mathcal{O}_L} g(x)\,\mathrm{d}x + \nu\mathcal{H}^1(\mathcal{O}_L)$$

Application for a test case

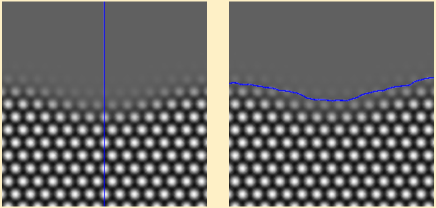

Combined model

$$E[\mathcal{O}_L, (\alpha_j, \mathcal{O}_j)_j] = \int\limits_{\mathcal{O}_L} g(x)\,\mathrm{d}x + \int\limits_{\Omega\setminus\mathcal{O}_L} (1 - g(x))\,\mathrm{d}x + \nu\mathcal{H}^1(\partial\mathcal{O}_L)$$

$$+ \eta \sum_{j=1,\cdots,n} \left(\int_{\mathcal{O}_j} f[\alpha_j](x)\,\mathrm{d}x + \frac{\nu}{2}\mathcal{H}^1(\partial\mathcal{O}_j) \right) .$$

Combined model

universitätbonn

$$E[\mathcal{O}_L, (\alpha_j, \mathcal{O}_j)_j] = \int_{\mathcal{O}_L} g(x)\,\mathrm{d}x + \int_{\Omega \setminus \mathcal{O}_L} (1 - g(x))\,\mathrm{d}x + \nu \mathcal{H}^1(\partial \mathcal{O}_L)$$
$$+ \eta \sum_{j=1,\cdots,n} \left(\int_{\mathcal{O}_j} f[\alpha_j](x)\,\mathrm{d}x + \frac{\nu}{2} \mathcal{H}^1(\partial \mathcal{O}_j) \right).$$

Result on PFC data

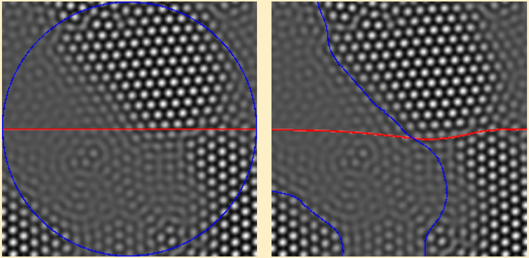

[Berkels, Rätz, R., Voigt '06]

Elastically stressed lattices

universitätbonn

description of a deformed lattice:

$\psi(x)$	atom position
ψ	elastic deformation
$\psi(x+M(\alpha)q_i)$	neighbor position

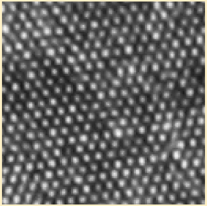

lattice pattern

local lattice classification function:

$$f[\alpha,\psi](x) = \frac{d^2}{m\,r^2}\chi_{[u>\theta]}(\psi(x)) \cdot \sum_{i=1}^{m}(1-\chi_{[u>\theta]}\psi(x+M(\alpha)q_i))$$

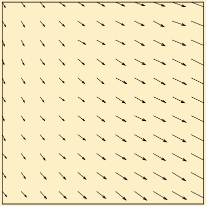

underlying deformation

The single crystal case

we have to deal with two types of deformations:

- the observer transformation induced by $M(\alpha)$

The single crystal case

we have to deal with two types of deformations:

- the observer transformation induced by $M(\alpha)$
- the actual lattice deformation $\psi(\cdot)$

The single crystal case

we have to deal with two types of deformations:

- the observer transformation induced by $M(\alpha)$
- the actual lattice deformation $\psi(\cdot)$

We are interested in the elastic deformation up to rigid body motions, hence we consider the following functional to be minimized for a single crystal:

$$E_{\mathsf{single}}[\alpha, \psi] \quad = \quad \int_\Omega f[\alpha, \psi](x)\,\mathrm{d}x$$

The single crystal case

we have to deal with two types of deformations:

- the observer transformation induced by $M(\alpha)$
- the actual lattice deformation $\psi(\cdot)$

We are interested in the elastic deformation up to rigid body motions, hence we consider the following functional to be minimized for a single crystal:

$$\begin{aligned} E_{\mathsf{single}}[\alpha,\psi] &= \int_\Omega f[\alpha,\psi](x)\,\mathrm{d}x + \mu E_{\mathsf{elast}}[\psi]\,, \\ \text{with } E_{\mathsf{elast}}[\alpha,\psi] &= \frac{1}{2}\int_{\mathcal{D}} \left|D\psi(x) + D\psi(x)^T - 2\,\mathbb{1}\right|^2 \mathrm{d}x \end{aligned}$$

under the constraint for the angular momentum

$\int_\Omega \psi_2(x)x_1 - \psi_1(x)x_2\,\mathrm{d}x = 0\,.$

[Berkels, Rätz, R., Voigt '07]

Concentration of energy at the minimizer

consider the Euler Lagrange equations:

Concentration of energy at the minimizer

consider the Euler Lagrange equations:

For ψ on $[u \circ \psi \neq 0]$:

$$-2\mu(\Delta\psi(x) + \nabla \operatorname{div} \psi(x)) = \lambda \begin{pmatrix} 0 & -1 \\ 1 & 0 \end{pmatrix} x \,,$$

where λ is a Lagrange multiplier reflecting the constraint.

Concentration of energy at the minimizer

consider the Euler Lagrange equations:

For ψ on $[u \circ \psi \neq 0]$:

$$-2\mu(\Delta\psi(x) + \nabla \operatorname{div} \psi(x)) = \lambda \begin{pmatrix} 0 & -1 \\ 1 & 0 \end{pmatrix} x \,,$$

where λ is a Lagrange multiplier reflecting the constraint.

For ψ on $[u \circ \psi = 0]$:

$$\big[(D\psi^T + D\psi) \cdot \nu\big] = \frac{d^2 \nabla u \circ \psi}{2m\mu r^2} \sum_{i=1}^{m} \Big(1 - H(u \circ \psi(\cdot + M(\alpha)q_i) - \theta) \\ - H(u \circ \psi(\cdot - M(\alpha)q_i) - \theta)\Big)$$

Concentration of energy at the minimizer

consider the Euler Lagrange equations:

For ψ on $[u \circ \psi \neq 0]$:

$$-2\mu(\Delta\psi(x) + \nabla \operatorname{div} \psi(x)) = \lambda \begin{pmatrix} 0 & -1 \\ 1 & 0 \end{pmatrix} x \,,$$

where λ is a Lagrange multiplier reflecting the constraint.

For ψ on $[u \circ \psi = 0]$:

$$\left[(D\psi^T + D\psi) \cdot \nu\right] = \frac{d^2 \nabla u \circ \psi}{2m\mu r^2} \sum_{i=1}^{m} \Big(1 - H(u \circ \psi(\cdot + M(\alpha)q_i) - \theta) - H(u \circ \psi(\cdot - M(\alpha)q_i) - \theta)\Big)$$

For the orientation α:

$$0 = \sum_{i=1}^{m} M'(\alpha) q_i \cdot \int_{[u\circ\psi=\theta]} H(u \circ \psi(\cdot - M(\alpha)q_i) - \theta) D\psi^T \nabla u \circ \psi \, \mathrm{d}\mathcal{H}^1 \,,$$

where $M'(\alpha) = \begin{pmatrix} 0 & -1 \\ 1 & 0 \end{pmatrix} M(\alpha)\,.$

Regularization and numerical relaxation

regularized lattice classification function:

$$f_\epsilon[\alpha,\psi] = \frac{d^2}{mr^2} H_\epsilon(u\circ\psi-\theta) \sum_{i=1}^{m} (1 - (H_\epsilon(u(\psi(\cdot + M(\alpha)q_i)) - \theta)))$$

regularized single grain energy:

$$E^\epsilon_{single}[\alpha,\psi] = \int_\Omega f_\epsilon[\alpha,\psi](x)\,\mathrm{d}x + \mu E_{\mathsf{elast}}[\psi]$$

Regularization and numerical relaxation

regularized lattice classification function:

$$f_\epsilon[\alpha,\psi] = \frac{d^2}{mr^2} H_\epsilon(u\circ\psi-\theta)\sum_{i=1}^{m}\left(1-\left(H_\epsilon(u(\psi(\cdot+M(\alpha)q_i))-\theta)\right)\right)$$

regularized single grain energy:

$$E^\epsilon_{single}[\alpha,\psi] = \int_\Omega f_\epsilon[\alpha,\psi](x)\,\mathrm{d}x + \mu E_{\mathsf{elast}}[\psi]$$

and again a regularized descent now in the deformation ψ:

$$g(\tilde\psi^{k+1}-\psi^k,\zeta) \quad = \quad -\tau_\psi^k \partial_\psi E^\epsilon_{\mathsf{single}}[\alpha^k,\psi^k](\zeta) \quad \forall \text{variations } \zeta\,,$$

Regularization and numerical relaxation

regularized lattice classification function:

$$f_\epsilon[\alpha,\psi] = \frac{d^2}{mr^2} H_\epsilon(u\circ\psi-\theta)\sum_{i=1}^{m}(1-(H_\epsilon(u(\psi(\cdot+M(\alpha)q_i))-\theta)))$$

regularized single grain energy:

$$E^{\epsilon}_{single}[\alpha,\psi] = \int_\Omega f_\epsilon[\alpha,\psi](x)\,\mathrm{d}x + \mu E_{\mathsf{elast}}[\psi]$$

and again a regularized descent now in the deformation ψ:

$$\begin{aligned} g(\tilde{\psi}^{k+1}-\psi^k,\zeta) &= -\tau_\psi^k \partial_\psi E^{\epsilon}_{\mathsf{single}}[\alpha^k,\psi^k](\zeta) \quad \forall \text{variations } \zeta\,,\\ \psi^{k+1} &= \tilde{\psi}^{k+1} - S(\cdot - x_\Omega)\,,\\ \text{where} \qquad S &= \frac{1}{2|\Omega|}\int_\Omega D\tilde{\psi}^{k+1} - (D\tilde{\psi}^{k+1})^T\,\mathrm{d}x\,,\; x_\Omega = \frac{1}{|\Omega|}\int_\Omega \mathrm{d}x\,, \end{aligned}$$

Regularization and numerical relaxation

regularized lattice classification function:

$$f_\epsilon[\alpha,\psi] = \frac{d^2}{mr^2} H_\epsilon(u\circ\psi-\theta) \sum_{i=1}^{m} (1-(H_\epsilon(u(\psi(\cdot+M(\alpha)q_i))-\theta)))$$

regularized single grain energy:

$$E^\epsilon_{single}[\alpha,\psi] = \int_\Omega f_\epsilon[\alpha,\psi](x)\,\mathrm{d}x + \mu E_{\mathsf{elast}}[\psi]$$

and again a regularized descent now in the deformation ψ:

$$\begin{aligned} g(\tilde\psi^{k+1}-\psi^k,\zeta) &= -\tau^k_\psi \partial_\psi E^\epsilon_{\mathsf{single}}[\alpha^k,\psi^k](\zeta) \quad \forall \text{variations } \zeta\,, \\ \psi^{k+1} &= \tilde\psi^{k+1} - S(\cdot - x_\Omega)\,, \\ \text{where} \qquad S &= \frac{1}{2|\Omega|}\int_\Omega D\tilde\psi^{k+1} - (D\tilde\psi^{k+1})^T\,\mathrm{d}x\,,\; x_\Omega = \frac{1}{|\Omega|}\int_\Omega \mathrm{d}x\,, \\ \alpha^{k+1} &= \alpha^k - \tau^k_\alpha \partial_\alpha E^\epsilon_{\mathsf{single}}[\alpha^k,\psi^{k+1}]\,. \end{aligned}$$

Regularization and numerical relaxation

regularized lattice classification function:

$$f_\epsilon[\alpha,\psi] = \frac{d^2}{mr^2} H_\epsilon(u\circ\psi-\theta)\sum_{i=1}^{m}(1-(H_\epsilon(u(\psi(\cdot+M(\alpha)q_i))-\theta)))$$

regularized single grain energy:

$$E^\epsilon_{single}[\alpha,\psi] = \int_\Omega f_\epsilon[\alpha,\psi](x)\,\mathrm{d}x + \mu E_{\mathsf{elast}}[\psi]$$

and again a regularized descent now in the deformation ψ:

$$\begin{aligned} g(\tilde\psi^{k+1}-\psi^k,\zeta) &= -\tau_\psi^k \partial_\psi E^\epsilon_{\mathsf{single}}[\alpha^k,\psi^k](\zeta) \quad \forall \text{variations } \zeta\,, \\ \psi^{k+1} &= \tilde\psi^{k+1} - S(\cdot - x_\Omega)\,, \\ \text{where} \qquad S &= \frac{1}{2|\Omega|}\int_\Omega D\tilde\psi^{k+1} - (D\tilde\psi^{k+1})^T\,\mathrm{d}x\,,\ x_\Omega = \frac{1}{|\Omega|}\int_\Omega \mathrm{d}x\,, \\ \alpha^{k+1} &= \alpha^k - \tau_\alpha^k \partial_\alpha E^\epsilon_{\mathsf{single}}[\alpha^k,\psi^{k+1}]\,. \end{aligned}$$

and $g(\zeta_1,\zeta_2) = \int_{\mathcal{D}} \zeta_1(x)\cdot\zeta_2(x) + \frac{\sigma^2}{2} D\zeta_1(x) : D\zeta_2(x)\,\mathrm{d}x$

Application for the single grain functional

test case (first row) and real data:

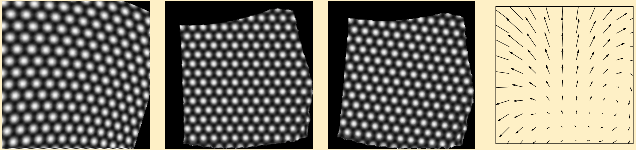

Application for the single grain functional

test case (first row) and real data:

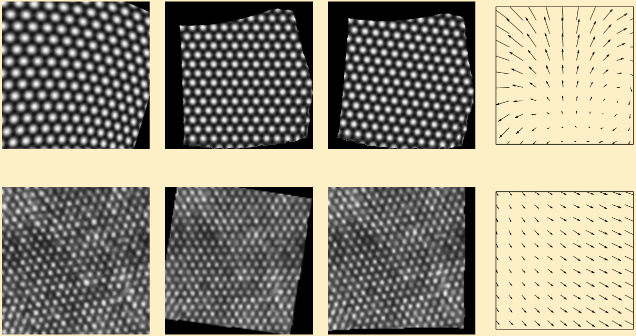

Application for the single grain functional

test case (first row) and real data:

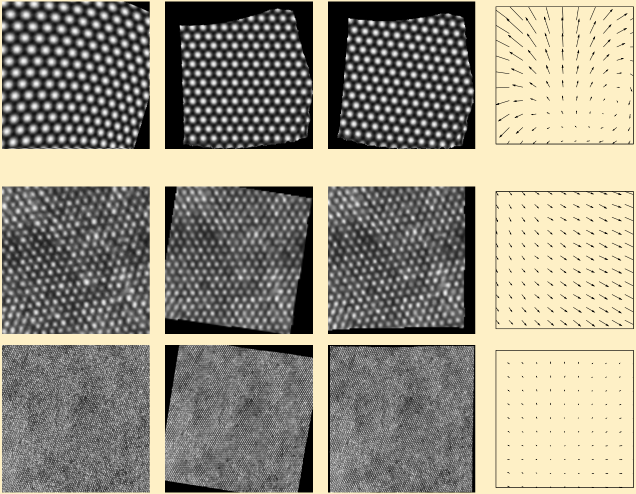

courtesy: N. Schryvers (Antwerpen University)

Combined model for elastically deformed grains

joint functional for $(\alpha_j, \mathcal{O}_j)_{j=1,\cdots,n}$ and ψ:

$$E_{\mathsf{joint}}[(\alpha_j, \Omega_j)_{j=1,\cdots,n}, \psi] \quad := \quad \sum_{j=1,\cdots,n} \big(E_{\Omega_j}[\alpha_j, \psi] + \eta \mathsf{Per}(\Omega_j)\big) + \mu\, E_{\mathsf{elast}}[\psi]$$

Combined model for elastically deformed grains

universitätbonn

joint functional for $(\alpha_j, \mathcal{O}_j)_{j=1,\cdots,n}$ and ψ:

$$E_{\text{joint}}[(\alpha_j, \Omega_j)_{j=1,\cdots,n}, \psi] \quad := \quad \sum_{j=1,\cdots,n} \big(E_{\Omega_j}[\alpha_j, \psi] + \eta \mathrm{Per}(\Omega_j) \big) \\ + \mu \, E_{\text{elast}}[\psi]$$

regularized functional in the two grain case:

$$E^{\delta,\epsilon}_{\text{joint}}[\alpha_1, \alpha_2, \phi, \psi] \quad := \quad \int_\Omega H_\delta(\phi) f_\epsilon[\alpha_2, \psi] + (1 - H_\delta(\phi)) f_\epsilon[\alpha_1, \psi] \\ + \nu |\nabla H_\delta(\phi)| \, \mathrm{d}x \\ + \frac{\mu}{2} \int_{\mathcal{D}} \left| D\psi(x) + D\psi(x)^T - 2\, \mathbb{1} \right|^2 \mathrm{d}x \, .$$

Combined model for elastically deformed grains (cont.)

Applications for a test case and for real data:

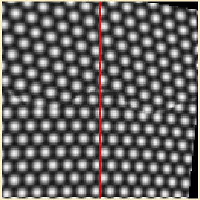
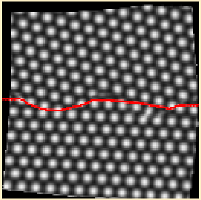
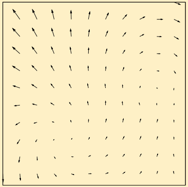

Combined model for elastically deformed grains (cont.)

Applications for a test case and for real data:

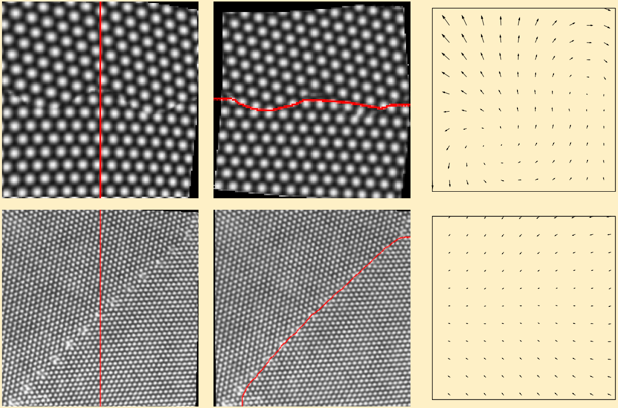

courtesy: N. Schryvers (Antwerpen University)

Outlook

- **Improving the model:**

- **Improving the model:**
  - considering the proper anisotropic elastic regularization:

$$C_{ijkl}(\alpha) = \sum_{\beta,\gamma,\delta,\eta} C^{ref}_{ijkl} M(\alpha)_{i\beta} M(\alpha)_{j\gamma} M(\alpha)_{k\delta} M(\alpha)_{l\eta},$$

where the C^{ref}_{ijkl}'s are priori known material parameters.

Outlook

- **Improving the model:**
  - considering the proper anisotropic elastic regularization:

$$C_{ijkl}(\alpha) = \sum_{\beta,\gamma,\delta,\eta} C_{ijkl}^{ref} M(\alpha)_{i\beta} M(\alpha)_{j\gamma} M(\alpha)_{k\delta} M(\alpha)_{l\eta},$$

    where the C_{ijkl}^{ref}'s are priori known material parameters.
  - evaluation of realistic macroscopic stresses

$$C_{ijkl}(\alpha) \frac{\nabla\psi + (\nabla\psi)^T}{2}$$

Outlook

- **Improving the model:**
  - considering the proper anisotropic elastic regularization:

$$C_{ijkl}(\alpha) = \sum_{\beta,\gamma,\delta,\eta} C_{ijkl}^{ref} M(\alpha)_{i\beta} M(\alpha)_{j\gamma} M(\alpha)_{k\delta} M(\alpha)_{l\eta},$$

    where the C_{ijkl}^{ref}'s are priori known material parameters.
  - evaluation of realistic macroscopic stresses

$$C_{ijkl}(\alpha)\frac{\nabla\psi + (\nabla\psi)^T}{2}$$

- **studying the dynamics of grain boundaries**

Outlook

- **Improving the model:**
  - considering the proper anisotropic elastic regularization:

$$C_{ijkl}(\alpha) = \sum_{\beta,\gamma,\delta,\eta} C^{ref}_{ijkl} M(\alpha)_{i\beta} M(\alpha)_{j\gamma} M(\alpha)_{k\delta} M(\alpha)_{l\eta},$$

    where the C^{ref}_{ijkl}'s are priori known material parameters.
  - evaluation of realistic macroscopic stresses

$$C_{ijkl}(\alpha)\frac{\nabla\psi + (\nabla\psi)^T}{2}$$

- **studying the dynamics of grain boundaries**
- **joining image aquisition and image processing**

A related two scale problem

A related two scale problem

Given: image u_0 dominated by right angle structures

u_0

A related two scale problem

Given: image u_0 dominated by right angle structures
we ask for a cartoon u and an anisotropic classification α.

u_0

A related two scale problem

Given: image u_0 dominated by right angle structures
we ask for a cartoon u and an anisotropic classification α.

u_0

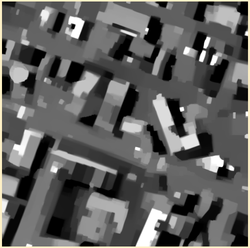

u

A related two scale problem

Given: image u_0 dominated by right angle structures
we ask for a cartoon u and an anisotropic classification α.

u_0

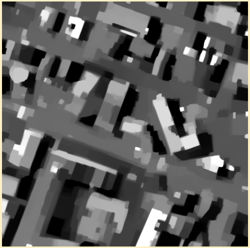

u

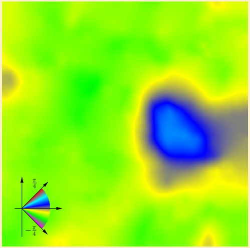

α

A related two scale problem

Given: image u_0 dominated by right angle structures
we ask for a cartoon u and an anisotropic classification α.

u_0

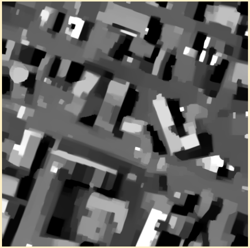

u

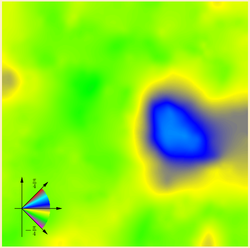

α

$\longrightarrow$ Joint extraction and orientation classification

Recall: the classical ROF model

Minimizing

$$E[u] := \frac{\lambda}{2} \int_\Omega (u_0 - u)^2 \, \mathrm{d}x + \int_\Omega |\nabla u|_2 \, \mathrm{d}x$$

gives a cartoon of u_0. Here $|x|_2 = \sqrt{x_1^2 + x_2^2}$.

[Rudin, Osher, Fatemi '92]

Recall: the classical ROF model

Minimizing

$$E[u] := \frac{\lambda}{2} \int_\Omega (u_0 - u)^2 \,\mathrm{d}x + \int_\Omega |\nabla u|_2 \,\mathrm{d}x$$

gives a cartoon of u_0. Here $|x|_2 = \sqrt{x_1^2 + x_2^2}$.

[Rudin, Osher, Fatemi '92]

Example

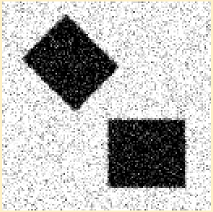

Original

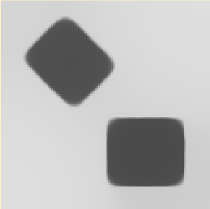

Reconstruction

The anisotropic ROF model

Given an anisotropy γ, minimizing

$$E_\gamma[u] := \frac{\lambda}{2}\int_\Omega (u_0 - u)^2 \,\mathrm{d}x + \int_\Omega \gamma(\nabla u)\,\mathrm{d}x$$

[Clarenz, Dziuk, R. '02], [Esedoglu, Osher '03]

The anisotropic ROF model

Given an anisotropy γ, minimizing

$$E_\gamma[u] := \frac{\lambda}{2}\int_\Omega (u_0 - u)^2 \,\mathrm{d}x + \int_\Omega \gamma(\nabla u)\,\mathrm{d}x$$

[Clarenz, Dziuk, R. '02], [Esedoglu, Osher '03]

Example

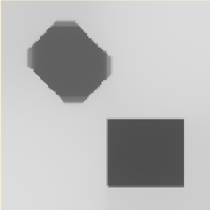

$\gamma = |\cdot|_1$

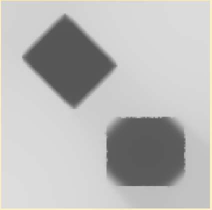

$\gamma = |\cdot|_1$ rot. by $\frac{\pi}{4}$

The anisotropic ROF model

universitätbonn

Given an anisotropy γ, minimizing

$$E_\gamma[u] := \frac{\lambda}{2}\int_\Omega (u_0 - u)^2 \,\mathrm{d}x + \int_\Omega \gamma(\nabla u)\,\mathrm{d}x$$

[Clarenz, Dziuk, R. '02], [Esedoglu, Osher '03]

Example

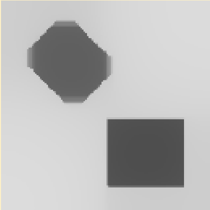

$\gamma = |\cdot|_1$

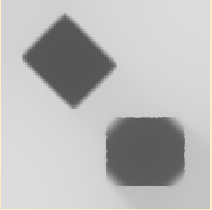

$\gamma = |\cdot|_1$ rot. by $\frac{\pi}{4}$

$\longrightarrow$ let γ depend on a coarse scale orientation α

Defining the anisotropic energy

$$E_\gamma[u,\alpha] := \frac{\lambda}{2}\int_\Omega |u_0(x) - u(x)|^2 \,\mathrm{d}x + \int_\Omega |M(\alpha(x))\nabla u(x)|_1 \,\mathrm{d}x,$$

where $M(\alpha) := \begin{pmatrix} \cos\alpha & \sin\alpha \\ -\sin\alpha & \cos\alpha \end{pmatrix}$ (rotation by $-\alpha$)

Defining the anisotropic energy

$$E_\gamma[u,\alpha] := \frac{\lambda}{2}\int_\Omega |u_0(x)-u(x)|^2\,\mathrm{d}x + \int_\Omega |M(\alpha(x))\nabla u(x)|_1\,\mathrm{d}x,$$

where $M(\alpha) := \begin{pmatrix} \cos\alpha & \sin\alpha \\ -\sin\alpha & \cos\alpha \end{pmatrix}$ (rotation by $-\alpha$)

Sample result of the final method

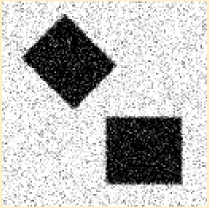

u_0

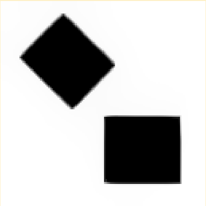

u

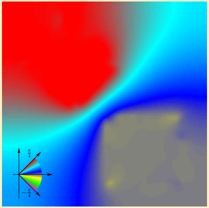

α

Regularization energy

Recall: The method shall be able to reconstruct corners

Regularization energy

Recall: The method shall be able to reconstruct corners
$\longrightarrow$ corners are co-dimension two objects

Regularization energy

Recall: The method shall be able to reconstruct corners
$\longrightarrow$ corners are co-dimension two objects
$\longrightarrow$ Simple Dirichlet type regularization not sufficient.

Regularization energy

Recall: The method shall be able to reconstruct corners
$\longrightarrow$ corners are co-dimension two objects
$\longrightarrow$ Simple Dirichlet type regularization not sufficient.

$$E_\alpha[\alpha] := \frac{1}{2}\int_\Omega \left(\mu_1|\nabla\alpha|^2 + \mu_2|\Delta\alpha|^2\right) \, \mathrm{d}x.$$

Regularization energy

Recall: The method shall be able to reconstruct corners
$\to$ corners are co-dimension two objects
$\to$ Simple Dirichlet type regularization not sufficient.

$$E_\alpha[\alpha] := \frac{1}{2}\int_\Omega \left(\mu_1|\nabla\alpha|^2 + \mu_2|\Delta\alpha|^2\right)\ \mathrm{d}x.$$

Final model:

$$E[u,\alpha] = \quad \int_\Omega \tfrac{\lambda}{2}|u_0 - u|^2 + |M(\alpha)\nabla u|_1 \ \mathrm{d}x + E_\alpha[\alpha].$$

Postprocessing by Bregman iteration

Reconstruction with zero to two Bregman iterations:

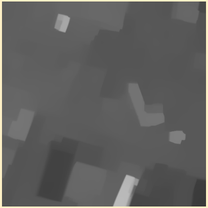

Postprocessing by Bregman iteration

Reconstruction with zero to two Bregman iterations:

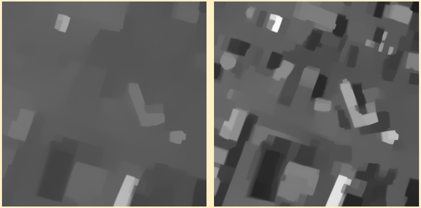

Postprocessing by Bregman iteration

Reconstruction with zero to two Bregman iterations:

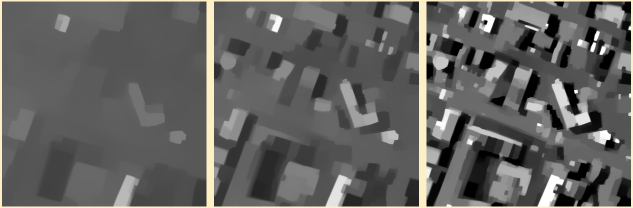

Postprocessing by Bregman iteration

Reconstruction with zero to two Bregman iterations:

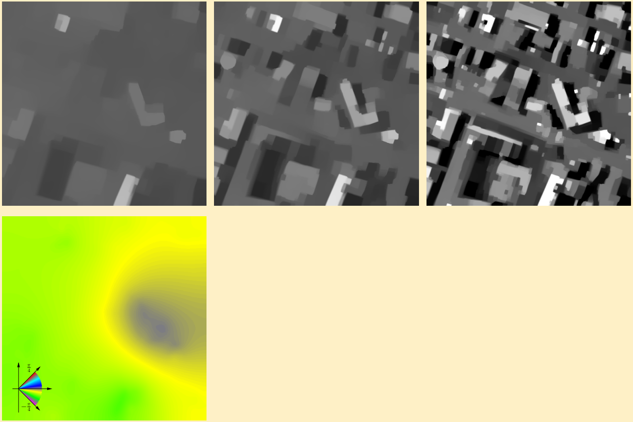

Postprocessing by Bregman iteration

Reconstruction with zero to two Bregman iterations:

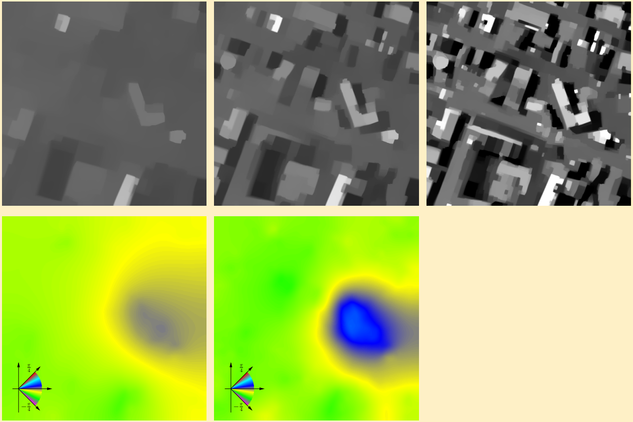

Postprocessing by Bregman iteration

Reconstruction with zero to two Bregman iterations:

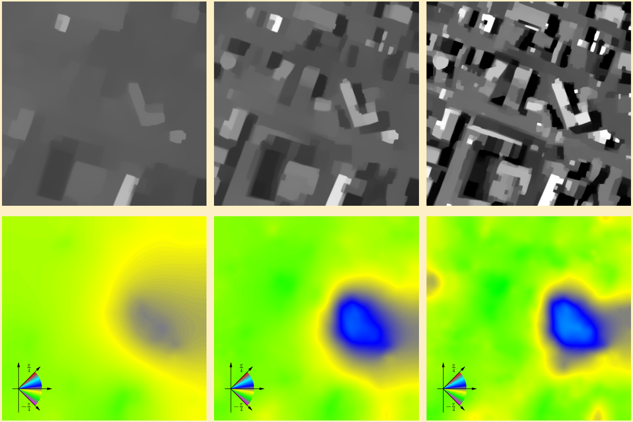

Reconstruction of a corner test data set

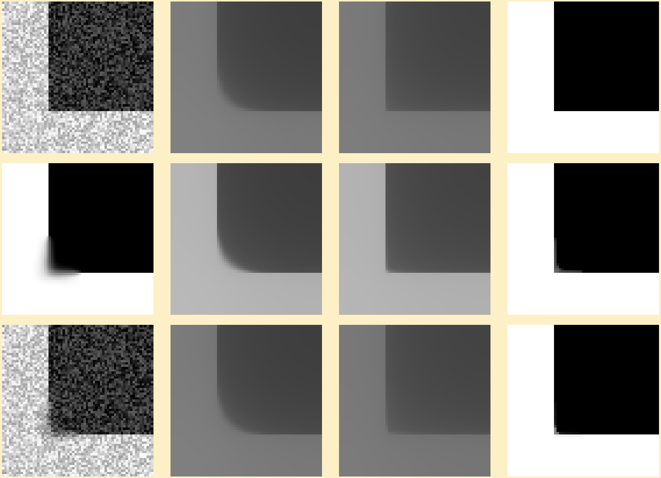

From left to right: Original images, isotropic reconstruction, anisotropic reconstruction with zero/two Bregman iterations

Application on aerial images

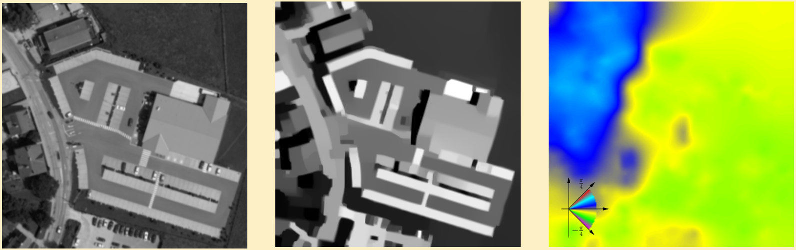

u_0 u α

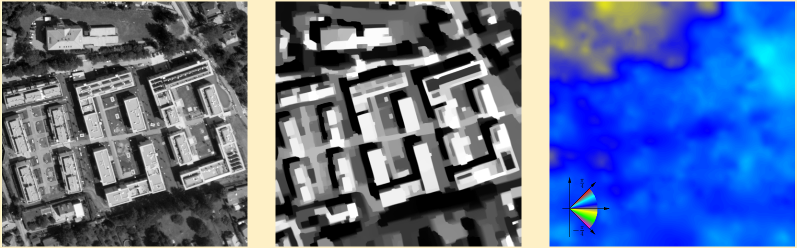

Application on aerial images (cont.)

u_0

u

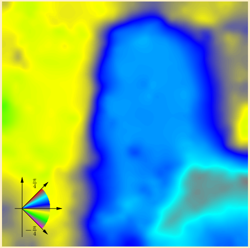

α

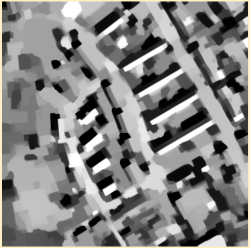

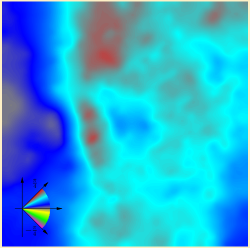

Generalization to orientation and shear

include a shearing transformation:

$$M_S(\beta) = \begin{pmatrix} \frac{\cos\beta}{\sin\beta} & 1 \\ \frac{1}{\sin\beta} & 0 \end{pmatrix}$$

Generalization to orientation and shear

include a shearing transformation:

$$\begin{aligned} M_S(\beta) &= \begin{pmatrix} \frac{\cos\beta}{\sin\beta} & 1 \\ \frac{1}{\sin\beta} & 0 \end{pmatrix} \\ M(\alpha,\beta) &= M(\alpha)M_S(\beta) \\ &= \begin{pmatrix} \frac{\cos\alpha\cos\beta+\sin\alpha}{\sin\beta} & \cos\alpha \\ \frac{\cos\alpha-\sin\alpha\cos\beta}{\sin\beta} & -\sin\beta \end{pmatrix} \end{aligned}$$

generalized model:

$$\begin{aligned} E[u,\alpha,\beta] &= \int_\Omega \frac{\lambda}{2}|u_0-u|^2 + |M(\alpha,\beta)\nabla u|_1 \,\mathrm{d}x \\ &\quad +E_\alpha[\alpha] + E_\beta[\beta]. \end{aligned}$$

Generalization to orientation and shear (cont.)

first numerical results:

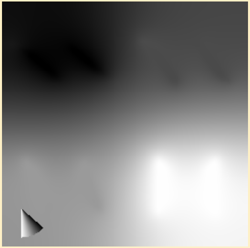

β